Three-dimensional scanning microscopy through thin turbid media

Xin Yang,[1] Chia-Lung Hsieh,[1,2] Ye Pu,[1,*] and Demetri Psaltis[1]

[1]*Optics Laboratory, Ecole Polytechnique Frederale de Lausanne (EPFL), Lausanne, 1015, Switzerland*
[2]*Department of Electrical Engineering, California Institute of Technology, 1200 East California Boulevard, MC 136-93, Pasadena, California 91125, USA*
[*]*ye.pu@epfl.ch*

Abstract: We demonstrate three-dimensional imaging through a thin turbid medium using digital phase conjugation of the second harmonic signal emitted from a beacon nanoparticle. The digitally phase-conjugated focus scans the volume in the vicinity of its initial position through numerically manipulated phase patterns projected onto the spatial light modulator. Accurate three dimensional images of a fluorescent sample placed behind a turbid medium are obtained.

OCIS codes: (070.5040) Phase conjugation; (090.1995) Digital holography; (110.0113) Imaging through turbid media; (160.4236) Nanomaterials; (180.6900) Three-dimensional microscopy.

References and links

1. E. N. Leith and J. Upatniek, "Holographic Imagery through Diffusing Media," J. Opt. Soc. Am. **56**(4), 523–523 (1966).
2. H. Kogelnik and K. S. Pennington, "Holographic Imaging Through a Random Medium," J. Opt. Soc. Am. **58**(2), 273–274 (1968).
3. Z. Yaqoob, D. Psaltis, M. S. Feld, and C. H. Yang, "Optical phase conjugation for turbidity suppression in biological samples," Nat. Photonics **2**(2), 110–115 (2008).
4. F. Lemoult, G. Lerosey, J. de Rosny, and M. Fink, "Manipulating spatiotemporal degrees of freedom of waves in random media," Phys. Rev. Lett. **103**(17), 173902 (2009).
5. M. Cui, E. J. McDowell, and C. H. Yang, "An in vivo study of turbidity suppression by optical phase conjugation (TSOPC) on rabbit ear," Opt. Express **18**(1), 25–30 (2010).
6. M. Cui and C. H. Yang, "Implementation of a digital optical phase conjugation system and its application to study the robustness of turbidity suppression by phase conjugation," Opt. Express **18**(4), 3444–3455 (2010).
7. C. L. Hsieh, Y. Pu, R. Grange, G. Laporte, and D. Psaltis, "Imaging through turbid layers by scanning the phase conjugated second harmonic radiation from a nanoparticle," Opt. Express **18**(20), 20723–20731 (2010).
8. C. L. Hsieh, Y. Pu, R. Grange, and D. Psaltis, "Digital phase conjugation of second harmonic radiation emitted by nanoparticles in turbid media," Opt. Express **18**(12), 12283–12290 (2010).
9. S. Popoff, G. Lerosey, M. Fink, A. C. Boccara, and S. Gigan, "Image transmission through an opaque material," Nat. Commun. **1**, (2010).
10. S. M. Popoff, G. Lerosey, R. Carminati, M. Fink, A. C. Boccara, and S. Gigan, "Measuring the transmission matrix in optics: an approach to the study and control of light propagation in disordered media," Phys. Rev. Lett. **104**(10), 100601 (2010).
11. I. M. Vellekoop and C. M. Aegerter, "Scattered light fluorescence microscopy: imaging through turbid layers," Opt. Lett. **35**(8), 1245–1247 (2010).
12. J. Aulbach, B. Gjonaj, P. M. Johnson, A. P. Mosk, and A. Lagendijk, "Control of light transmission through opaque scattering media in space and time," Phys. Rev. Lett. **106**(10), 103901 (2011).
13. O. Katz, E. Small, Y. Bromberg, and Y. Silberberg, "Focusing and compression of ultrashort pulses through scattering media," Nat. Photonics **5**(6), 372–377 (2011).
14. D. J. McCabe, A. Tajalli, D. R. Austin, P. Bondareff, I. A. Walmsley, S. Gigan, and B. Chatel, "Spatio-temporal focusing of an ultrafast pulse through a multiply scattering medium," Nat. Commun. **2**, (2011).
15. J. W. Goodman, W. H. Huntley, D. W. Jackson, and M. Lehmann, "Wavefront-Reconstruction Imaging through Random Media - (Resolution Limitations - Atmospheric Effects - E/T)," Appl. Phys. Lett. **8**(12), 311–313 (1966).
16. S. C. Feng, C. Kane, P. A. Lee, and A. D. Stone, "Correlations and fluctuations of coherent wave transmission through disordered media," Phys. Rev. Lett. **61**(7), 834–837 (1988).

#158559 - $15.00 USD Received 22 Nov 2011; revised 10 Jan 2012; accepted 11 Jan 2012; published 19 Jan 2012

1. Introduction

The formation of a focus through a medium containing randomly dispersed scatters, known as turbid or disordered medium, proves to be difficult because the initial wave front is rapidly destroyed or "forgotten" inside the medium by the multiple scatterings. Driven by the need for non-invasive optical imaging in biological tissues, which remains a great challenge to modern science and technology, intensive efforts have been made in recent years to deliver a focus through turbid media [1–14]. These efforts have shown that the information about the initial wave front, though highly scrambled, is not lost in the scattered field and can be retrieved by undoing the scattering process by propagating through the turbid medium itself.

Holography has a long history in scattering cancelation [15]. Exploiting the optical memory effect [16], we have previously demonstrated scanning microscopy using digital phase conjugation (DPC) to focus light through turbid media using Second Harmonic Radiation IMaging Probes (SHRIMPs) [7] as beacons. Similar use of the memory effect was also demonstrated earlier using an iterative focus optimization approach [11]. In both implementations, it was shown that once a focus is formed behind a turbid medium, the integrity of the focus is maintained even if the input wave front is modulated by a linear spatial phase shift or is rotated, resulting in a displaced focus. Here we show that the memory effect and the scanning capability can be extended to three dimensions by axially displacing the phase-conjugated focus using a quadratic phase modulation in the DPC. This technique is an important step toward three-dimensional scanning imaging in turbid media. It is also applicable to all the other focus-forming methods.

2. Experiments

The experimental setup is shown in Fig. 1. The DPC records the complex scattering through harmonic holography and subsequently generates a phase conjugated focus [8]. A 150 fs pulsed Ti:sapphire oscillator centered at 800 nm is used as the light source. The laser beam from the oscillator is divided into two arms by a polarization beam splitter (PBS). The signal arm is focused by a 10 × microscope objective (OBJ1, NA 0.25) onto a single SHRIMP, with a peak intensity of ~10^{12} W/cm^2. The SHG signal from the SHRIMP emits in both forward and backward directions. The backward SHG signal is imaged onto a charge-coupled device (CCD) camera (Scion, CFW-1312M, CCD1) by OBJ1 and L1. The forward SHG signal propagates through the turbid layer, and is then imaged onto an electron multiplying charge coupled device (EMCCD) camera (Andor iXonEM + 885, CCD2) by OBJ2 (10 × , NA 0.25) L2. The magnification of both imaging systems is ~12. The EMCCD is placed 20 cm away from the imaging plane of the SHRIMP sample to make full use of its active detection area, and the incident face of the turbid medium is placed on the imaging plane of the EMCCD. The reference arm is focused onto a beta-BaB_2O_4 (BBO) crystal, and the resultant SHG beam is collimated and sent to the EMCCD. The reference and signal beams are overlapped both spatially and temporally on the EMCCD with an angle of ~1 degree, and the complex field is then digitally reconstructed from the off-axis hologram. The non-interference background is digitally subtracted to make full use of the spatial frequency bandwidth for DPC.

We use 300 nm barium titanate ($BaTiO_3$) nanocrystals of tetragonal structure as SHRIMPs for harmonic holography recording. The $BaTiO_3$ nanocrystals are dispersed in methanol solvent and sonicated for 5 minutes to minimize particle clustering. The suspension is then dropped onto a microscope cover slip, and heated up at 100þC to evaporate the solvent. A microscope image shows that the SHRIMPs are evenly distributed on one side of the cover slip (data not shown). To demonstrate the concept of three-dimensional imaging, fluorescent beads (Cosperic, absorption ~400 nm, emission ~450 nm, 2-5 μm diameter distribution) are randomly deposited on both sides of the same SHRIMP-loaded cover slip (~170 μm thick) as the imaging targets (see the inset of Fig. 1). The turbid medium is composed of two layers of

#158559 - $15.00 USD Received 22 Nov 2011; revised 10 Jan 2012; accepted 11 Jan 2012; published 19 Jan 2012

single sided adhesive tape (Scotch, 3M) attached on a cover glass. Neglecting the absorption, the mean free path of the turbid medium is estimated to be ~3 μm at 400 nm wave length.

To produce the phase conjugated focus, the reconstructed phase information of the scattered field is digitally conjugated, and projected onto a phase-only reflective SLM (PLUTO-VIS, HOLOEYE). The pixel size of the SLM is 8 × 8 μm^2, which matches the pixel size of the EMCCD. In DPC, the collimated reference beam is directed to the SLM by adjusting the flip mirror (FM2), and it generates the phase conjugated beam after reflection. When the SLM and EMCCD are perfectly aligned pixel by pixel, the phase-conjugated beam propagates backward through exactly the same paths as the forward wave in the scattering medium, and thereby it cancels the scattering distortion and forms a clear focus at the SHRIMP's position. The focus is monitored by CCD1.

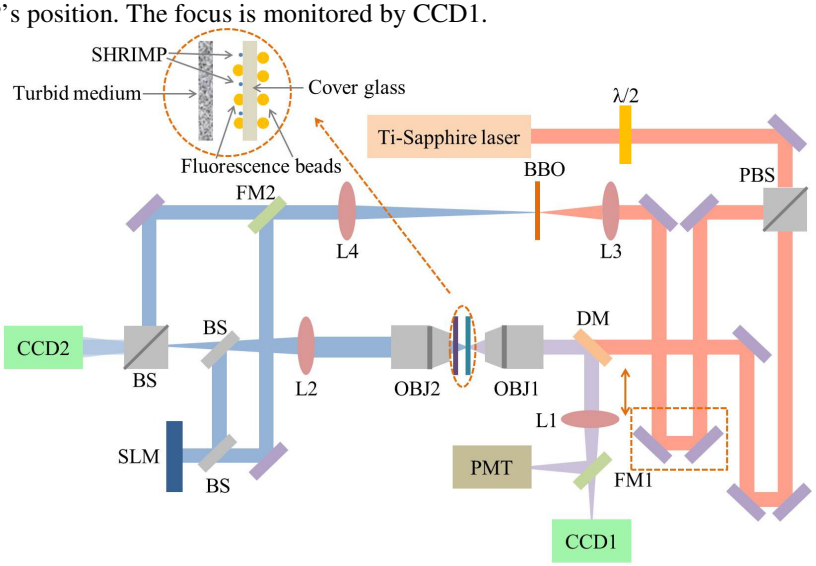

Fig. 1. Schematic diagram of the experimental setup. BS: non-polarization beam splitter; PBS: polarization beam splitter; FM1-FM2: flip mirror; DM: dichroic mirror; OBJ1-OBJ2: microscope objective; L1-L4: lens; λ/2: half wave plate. Inset: illustrative diagram of the SHRIMP, imaging targets and turbid medium.

Scanning of the phase-conjugated focus in all three dimensions is realized by digitally modifying the phase pattern projected onto the SLM. The SLM and turbid medium are configured on the conjugate planes of the imaging system, and there is no mechanical movement involved during the scanning process. Figure 2 shows the schematic concept of 3D digital scanning. In the transverse (x-y) direction, the focus shift is achieved by modulating the original phase-conjugated wave front with a linear spatial phase change, which results in a tilt of the wave front. The amount of the shift is determined by the angle of the tilt [Fig. 2(a)]. For a lateral shift of Δx in the x direction, the required modulation is $\exp\left(ik\, x\Delta x/z_0\right)$, where z_0 is the distance between the beacon position and the hologram recording plane in the object domain. In the axial (z) direction, we achieve the focus shift by modulating the phase conjugation wave front with a quadratic spatial phase change, which gives rise to a curvature in the wave front. The amount of the shift Δz is dependent on the curvature of the quadratic phase modulation [Fig. 2(b)], which is in the form of $\exp\left[ik\,\rho^2/R\right]$, where $\rho^2 = x^2 + y^2$, and $R = z_0\left(z_0 - \Delta z\right)/\Delta z$ is the curvature radius. Both raster-scanning and focusing at arbitrary locations in a volume (bounded by the range of scanning) can be accomplished through a combination of the two types of modulation. More specifically, assuming the original phase conjugated focus is located at the origin of the coordinates $(0,0,0)$, in order to move the

#158559 - $15.00 USD Received 22 Nov 2011; revised 10 Jan 2012; accepted 11 Jan 2012; published 19 Jan 2012

phase conjugated focus to $(\Delta x, \Delta y, \Delta z)$, the compound modulation should be $\exp\left[ik\left(x\Delta x + y\Delta y\right)/z_0\right]\exp\left[ik\,\rho^2/R\right]$. The coordinates (x, y) are on the plane just behind the scattering medium, while $(\Delta x, \Delta y)$ are the coordinates on the original SHRIMP plane. Here, the only parameter required in the calculation is the distance between the SHRIMP beacon and the turbid medium (z_0). Due to experimental constraints, certain geometric parameters cannot be measured accurately, and we therefore need to numerically adjust z_0 for best results. The scattering medium used in this experiment is single sided tapes attached on a cover glass. The thickness of the cover glass is taken into account when calculating the required phase modulation. The correctness of the calculated phase is verified in the same setup without the scattering medium. Finally, the scattering medium is inserted and three dimensional scanning through that medium is achieved.

In the imaging of the fluorescent beads, the fluorescence signal at ~450 nm wave length is collected by OBJ1 and sent to a photomultiplier tube (PMT) through L1 and FM1. The phase conjugated focus is scanned across the target by continuously projecting the pre-calculated phase pattern onto the SLM. A clear contrast is seen when the focus falls on the fluorescence beads. To minimize the detector noise from ambient light, the signal is modulated by a chopper at 330 Hz, and read out by a lock-in amplifier.

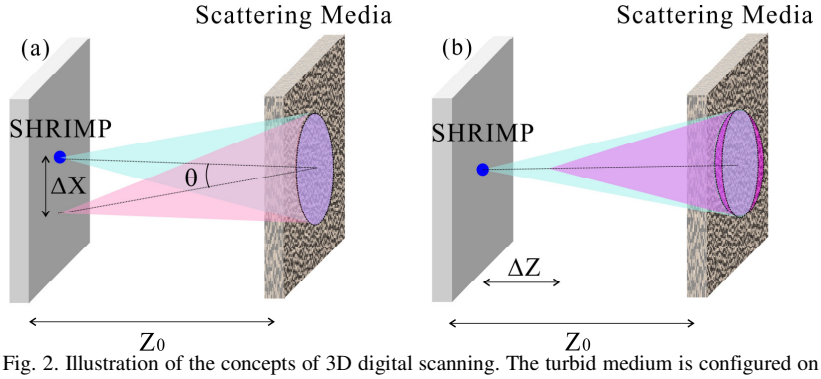

Fig. 2. Illustration of the concepts of 3D digital scanning. The turbid medium is configured on the image plane of the EMCCD/SLM. (a) The SHG wave emitted from the SHRIMP propagates through the turbid medium, and the resultant random wave front is recorded on the same plane. The phase information is conjugated, multiplied by a tilting wave front, and sent back through the turbid medium. The phase conjugated focus is displaced from the original position of SHRIMP in the x or y direction; (b) The SHG wave emitted from the SHRIMP propagates through the turbid medium, and the resultant random wave front is recorded on the same plane. The phase information is conjugated, multiplied by a quadratic wave front, and sent back through the turbid medium. The phase conjugated focus is displaced from the original position of SHRIMP in the z direction.

3. Results and discussions

The "memory effect" in the propagation of coherent waves through disordered media, as discovered by Feng et al [16], suggests that correlation exists between the emerging wave fronts from the disordered medium when the incident wave front changes slightly. They identified three types of correlations in the overall correlation, namely short-range, long-range, and infinite-range correlations, among which the short-range correlation is the dominant term. In particular, the short-range field correlation among the three types of correlations they discussed, $C_T\left(k\theta L\right) = k\theta L/\sinh\left(k\theta L\right)$ has laid out a sound foundation for the implementations of two-dimensional scanning microscopy through turbid medium by tilting the incident wave front. Here L is the thickness of scattering medium, and θ is the tilted angle [7, 11]. We use field correlation instead of intensity correlation for the convenience of the following discussion, and the intensity correlation can be obtained through

#158559 - $15.00 USD Received 22 Nov 2011; revised 10 Jan 2012; accepted 11 Jan 2012; published 19 Jan 2012

$C_T^2(k\theta L)$. To extend the scanning into three dimensions, we note that an axial displacement of the focus requires a quadratic phase modulation, which can be considered as composed of a set of plane waves in the spatial Fourier domain. The correlation function in the axial direction is thus obtained by summing up the correlation functions for each individual plane wave. We therefore write the axial correlation function as:

$$C_A(\Delta z) = \frac{\iint C_T(k\theta_x L) C_T(k\theta_y L) F_{\theta_x,\theta_y}\left\{\exp\left[ik\rho^2/R\right]\right\} d\theta_x d\theta_y}{\iint F_{\theta_x,\theta_y}\left\{\exp\left[ik\rho^2/R\right]\right\} d\theta_x d\theta_y} \qquad (1)$$

where F_{θ_x,θ_y} is a 2D Fourier transform from x-y to θ_x-θ_y.

In order to validate the axial correlation function, we measure the intensity of the phase conjugated focus as a function of the displacement, which is plotted in Fig. 3. Three scattering samples with one, two, and three layers of single sided adhesive tapes (Scotch, 3M) are used as the turbid medium. The axial coordinate is defined as the normalized intensity of the phase conjugated focus. The red, green, blue curves stand for the results of one, two, three scattering layers, respectively.

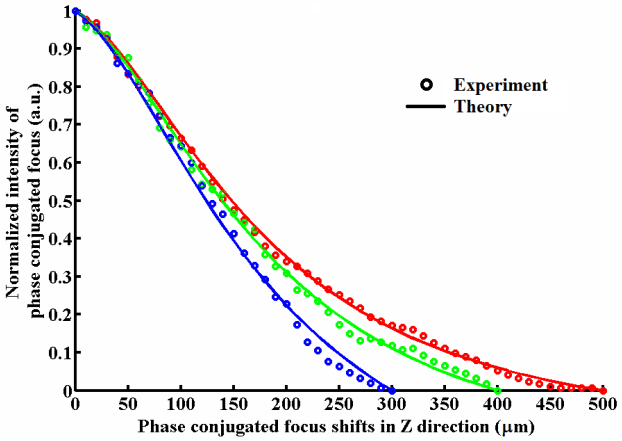

Fig. 3. Normalized intensity of phase conjugated focus verse shift distance in Z directions. red: one layer of single sided tape; green: two layers of single sided tape; blue: three layers of single sided tape.

In Fig. 3, we also plot theoretical calculations as solid curves for comparison. The calculation is based on numerical propagation of a spherical wave subject to the correlation function as an intensity modulation. The effective thicknesses of the turbid samples are estimated by fitting the curves to experimental data, which turns out to be ~20 μm, ~25 μm, and ~30 μm, for one, two, and three layers, respectively. The effective thicknesses of the scattering layer for the turbid samples are not proportional to their actual thicknesses, because the scattering effect of single sided tape mainly results from surface roughness. The range of the axial memory effect is a function of the thickness of the scattering layer and the distance between the focus and the turbid medium plane. From Fig. 3, this gives approximately 220 μm in the case of the thickest medium if the focus intensity above e^{-2} of the peak value is considered acceptable.

The three-dimensional imaging of fluorescent beads is shown in Fig. 4, where panels 4(a) and (c) show the microscope images of the scanning areas (~75×75 μm^2) of the two layers, panels 4(b) and (d) are the corresponding scanned images viewed through the turbid medium. Comparing the two groups of images, the fluorescence targets are clearly resolved in the scanned images, and the distributions of beads are well matched, confirming the validity of the approach. No meaningful image is found in the control experiment without DPC (data not shown). The scanning speed is limited by the refreshing rate of the SLM (60 Hz), and the

#158559 - $15.00 USD Received 22 Nov 2011; revised 10 Jan 2012; accepted 11 Jan 2012; published 19 Jan 2012

integration time (100 ms/pixel) of the lock in amplifier. The variation of fluorescence intensities between different beads is attributed to the size variation of the beads (2-5 μm in diameter) and the intensity drop of the focus at off-center locations. The gray scales in Fig. 4(b) and (d) have been normalized so that the brightest spot is white and the darkest spot is black. The absolute signal intensity of Fig. 4(d) is roughly half of that of Fig. 4(b), because the beads in Fig. 4(b) are located at the same plane as the beacon SHRIMP, while in the beads in Fig. 4(d) it is located 170μm away from the beacon. This is in accordance with the results shown in Fig. 3. Figure 4(e) shows the scanning image of a fluorescent bead in y-z plane along the dashed line in Fig. 4(a) and (c).

The resolution is limited by the spot size of the phase conjugated focus, i.e. point spread function (PSF) [Fig. 5]. The lateral and axial resolutions are ~2.5 μm [Fig. 5(a)] and ~35 μm [Fig. 5(b)], respectively, corresponding to an effective numerical aperture (NA) of ~0.1, which is considerably smaller than the NA = 0.25 of the microscope objective marked OBJ2 in Fig. 1. We believe this is due to the small incident beam width (W) projected on the disordered medium and hence the approximation that the scattering medium is infinite in the lateral dimension is no longer valid. This manifests itself as a system with reduced NA because some of the higher angular components of the light beam do not get properly phase conjugated. The resolution can be significantly improved with a redesigned optical system with much larger W. Additionally, both the lateral and axial resolutions change slightly when focusing on different planes, due to the optical geometry and the variations in the effective NA. This is reflected in the slightly different spot sizes of the phase conjugated foci. If the scanning range in the axial direction is larger, a more evident change in resolution would be observed.

We define the signal to noise ratio (SNR) of the phase conjugated scanned images [Fig. 4(b) and (d)] as the ratio between the average intensity at the signal spot over the standard deviation of the background area. The average SNRs measured as such are ~20 and ~16 for Fig. 4(b) and (d), respectively. We note that these results are achieved with a phase-only SLM. Provided a complex (amplitude and phase) SLM, the intensity of the diffusive background can be further suppressed for an improved SNR.

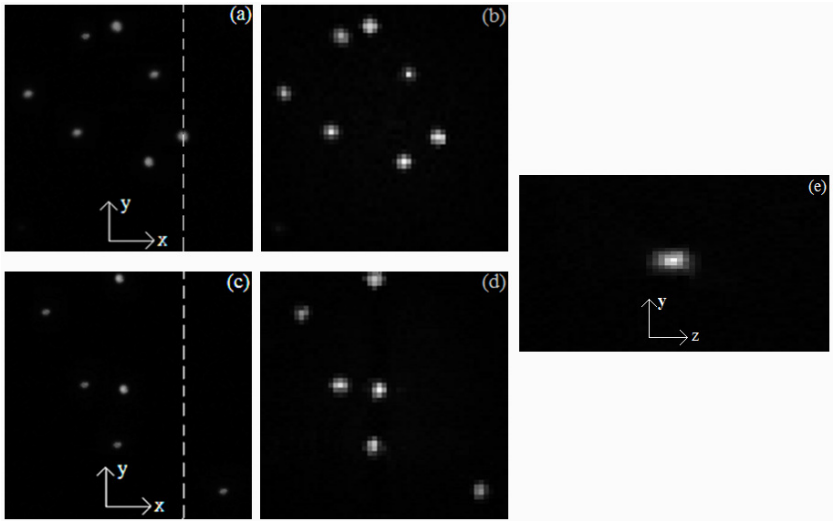

Fig. 4. (a) Microscope image and (b) Phase conjugated scanned microscope image of fluorescence beads deposited on the same plane as the SHRIMP; (c) Microscope image and (d) Phase conjugated scanning microscope image of fluorescence beads deposit on the plane ~170μm away from SHRIMP; (e) Scanned image of a Y-Z plane, which crosses the dotted line in Fig. 4 (a) and (c). (b) and (d) pixel size: 1.5 × 1.5μm^2, image size: 75 × 75μm^2; (e) pixel size: 1.5 × 10μm^2, image size: 75 × 500μm^2.

#158559 - $15.00 USD Received 22 Nov 2011; revised 10 Jan 2012; accepted 11 Jan 2012; published 19 Jan 2012

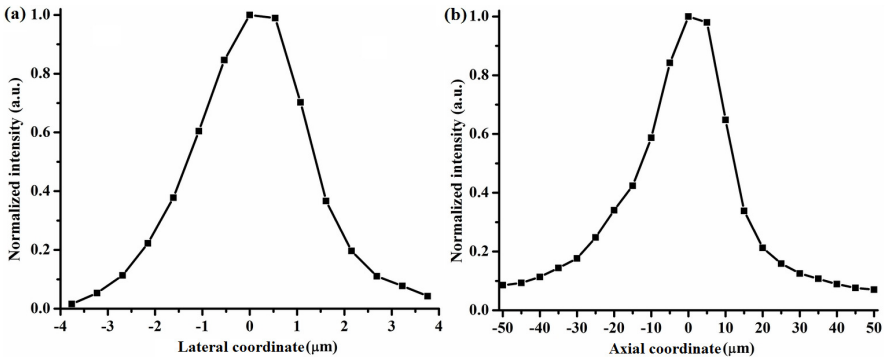

Fig. 5. Cross-section plot of the intensity of the phase conjugated focus: (a) Lateral direction; (b) Axial direction.

4. Conclusion

We have demonstrated three-dimensional phase conjugated scanning microscopy through turbid medium. Based on the optical memory effect, we show that the phase conjugated focus can be displaced from its original position in all three dimensions with controlled distance. We find that the scanning range in the longitudinal dimension is consistently larger compared to the transverse scanning range. This fundamental difference between transverse and longitudinal scanning will be explored further in a forthcoming publication. In the experiments, the scanning is achieved digitally by modulating the phase-conjugation pattern projected onto the phase-only SLM. Fluorescent beads of three dimensional distributions are used as the imaging target. The scanning images agree well with the wide-field images. This technique is adaptable to other imaging methods through turbid media such as wave front shaping, and provides the possibility for fast three dimensional imaging through thin biological tissue.

#158559 - $15.00 USD Received 22 Nov 2011; revised 10 Jan 2012; accepted 11 Jan 2012; published 19 Jan 2012